Cancer Letters 642 (2026) 218284

Contents lists available at ScienceDirect

Cancer Letters

journal homepage: www.elsevier.com/locate/canlet

# MEOX2 enhances DNA repair and therapy resistance in Glioblastoma stem-like cells via PARP1 interaction

Monia Russo [a,1], Elvia Valentini [b,1], Vincenza Aliperti [a], Federico Copparoni [a], Amanda Linkous [c], Claudia Montaldo [d], Silvia Soddu [e], Jean-Maxime Besson [f], Marie Lopez [f], Manuela Helmer Citterich [b], Alessandro Michienzi [a], Marco Tripodi [d,g], Silvia Anna Ciafrè [a,*], Silvia Galardi [b,**]

[a] Department of Biomedicine and Prevention, University of Rome Tor Vergata, Rome, Italy
[b] Department of Biology, University of Rome Tor Vergata, Rome, Italy
[c] Department of Pharmacology, Vanderbilt University, Nashville, TN, United States
[d] National Institute for Infectious Diseases L. Spallanzani, IRCCS, Rome, Italy
[e] Unit of Cellular Networks and Molecular Therapeutic Targets, Department of Research and Advanced Technologies, IRCCS Regina Elena National Cancer Institute, Rome, Italy
[f] Institut des Biomolécules Max Mousseron (IBMM), CNRS-UM-ENSCM, Montpellier, France
[g] Department of Molecular Medicine, Sapienza University of Rome, Rome, Italy

A B S T R A C T

The most widely accepted hypothesis for glioblastoma development posits that glioblastoma stem-like cells (GSCs) play a central role in tumor initiation, recurrence, and resistance to both chemotherapy and radiotherapy. We and others previously showed the importance of Mesenchyme Homeobox 2 (MEOX2) in supporting GSC survival and metabolism. In the present work, we demonstrate that MEOX2 also promotes DNA damage repair and contributes to resistance against genotoxic therapies in GSCs. Using a GLICO (GLioblastoma Cerebral Organoid) model, we show that MEOX2 knockdown impairs tumor growth and increases sensitivity to temozolomide (TMZ). Mechanistically, we find that MEOX2 depletion in 2D culture systems compromises genomic stability and impairs DNA repair. Co-immunoprecipitation and mass spectrometry analyses identified poly ADP-ribose polymerase 1 (PARP1) as a novel MEOX2 interactor. Consistent with this, MEOX2-depleted cells exhibit reduced PARylation levels and increased sensitivity to the PARP1 inhibitor Talazoparib, highlighting a potential therapeutic vulnerability.

Altogether, our findings reveal a previously unrecognized role for MEOX2 in the DNA damage response of GSCs, particularly in promoting survival and recovery after chemotherapy and ionizing radiation. These results also suggest that MEOX2 functions as a partner of PARP1 and may represent a promising therapeutic target in GBM.

## 1. Introduction

Glioblastoma (GBM) is a highly aggressive and currently incurable brain tumor, characterized by limited treatment options and dismal patient outcomes, despite the aggressive standard of care therapy, consisting of maximal surgical resection, fractionated radiotherapy, and chemotherapy with the DNA-alkylating agent, temozolomide (TMZ) [1].

Mesenchyme homeobox 2 (MEOX2), a transcription factor involved in mesodermal development, is markedly overexpressed in GBM, with elevated levels correlating with reduced survival, particularly in radiotherapy-resistant cases [2]. We and others previously showed that MEOX2 is strongly enriched in glioma stem-like cells (GSCs) [3,4], a therapy-refractory subpopulation responsible for tumor initiation, resistance to standard therapy, and recurrence [5]. In GSCs, MEOX2 is essential for maintaining self-renewal and viability, positioning it as a key regulator of GBM malignancy.

In the present work, we investigated the contribution of Meox2 to the repair of therapy-induced DNA damage in GSCs and in glioblastoma cerebral organoids. By co-immunoprecipitation and mass spectrometry, we searched for protein interactors of Meox2 that may be involved in DNA damage sensing and repair, and found PARP1, a major sensor of DNA double-strand breaks and a recruiter of repair proteins [6]. Consistently, we revealed an increased sensitivity of MEOX2 KD GSCs to

* Corresponding author.
** Corresponding author.
*E-mail addresses:* ciafre@uniroma2.it (S.A. Ciafrè), silvia.galardi@uniroma2.it (S. Galardi).
[1] These authors equally contributed to this work.

https://doi.org/10.1016/j.canlet.2026.218284
Received 9 September 2025; Received in revised form 19 January 2026; Accepted 24 January 2026
Available online 29 January 2026

**Abbreviations:**

| | |
|---|---|
| DDR | DNA damage response |
| GFP | green fluorescent protein |
| co-IP | co-immunoprecipitation |
| GBM | glioblastoma |
| GLICO | glioblastoma cerebral organoid |
| GSC | glioma stem-like cells |
| MEOX2 | mesenchyme homeobox 2 |
| IB | immunoblot |
| IP | immunoprecipitation |
| IR | ionizing radiation |
| PARP1 | poly ADP-ribose polymerase1 |
| PARylation | poly-ADP-ribosylation |
| TMZ | temozolomide |

the PARP1 inhibitor Talazoparib, thus highlighting a potential therapeutic vulnerability.

## 2. Materials and methods

All materials and methods employed to perform this study are described in detail in the Supplementary data.

## 3. Results and discussion

To further strengthen the biological relevance of our findings, we investigated MEOX2 function in the GLioblastoma Cerebral Organoid (GLICO) model – human embryonic stem cell-derived cerebral organoids containing GBM tumor cells. These advanced 3D models recapitulate early human brain development and provide a physiologically relevant context in which GBM cells phenocopy patient tumors [7,8].

We generated green fluorescent protein (GFP)-expressing GSCs with or without MEOX2 knockdown (shMEOX2 vs. shC) and confirmed a significant reduction in shMEOX2 cell viability under 2D culture conditions, consistent with prior results (Fig. S1A) [3]. Subsequently, we co-cultured shMEOX2 and shC cells with cerebral organoids. To evaluate invasion and tumor growth, we performed immunofluorescence microscopy for GFP and quantified the corrected total cell fluorescence in each organoid at Days 9 and 12. While no differences in invasion were observed at Day 9, clear differences emerged at Day 12 (Fig. 1A). These findings suggest that both control and shMEOX2 cells invade the organoids at comparable rates initially, but shMEOX2 cells fail to sustain growth over time.

Since a major challenge in GBM treatment is temozolomide (TMZ) resistance, we assessed TMZ sensitivity of shC and shMEOX2 cells in GLICO models (Fig. 1B). We observed that at 7 days post-treatment, TMZ significantly reduced the tumor growth of shMEOX2 GLICO model, whereas the growth of shC tumors was not significantly affected, indicating that MEOX2 can contribute to TMZ resistance. To assess TMZ-induced DNA damage [9], we quantified γH2AX/53BP1 co-localized foci via immunofluorescence in shC and shMEOX2 cells, with or without treatment. Co-localization was used to improve DNA damage response specificity, as γH2AX alone may appear in contexts unrelated to double-strand breaks [10,11]. As shown in Fig. 1C and Fig. S1B and 24 hours of TMZ treatment (100 μM) did not significantly increase the number of γH2AX/53BP1 foci in shC cells, whereas it led to a marked increase in the number of foci in shMEOX2 cells. At 48 h of treatment, the number of foci increased, compared to untreated cells, in both shC and shMEOX2 cells, and the difference between untreated and treated cells was greater in shMEOX2 compared to shC cells. Interestingly, the quantification of γH2AX/53BP1 foci reveals a trend toward an endogenous DNA damage in non-treated shMEOX2 cells, implicating MEOX2 in genome stability. In agreement with the lack of DNA damage at this dosage of TMZ, in shC cells we did not observe the G2/M cell cycle arrest typically associated with TMZ-induced DNA damage [11]. Conversely, in shMEOX2 cells, the increased DNA damage induced by TMZ was flanked by a significant arrest in G2/M (Fig. 1D–S1C). Thus, at doses where TMZ alone fails to induce DNA damage and the related cell cycle arrest, MEOX2 knockdown enables this response. Of note, our choice of this dosage (100 μM) of TMZ stems from our observations about the resistance of the selected GSC models to lower concentrations of this drug (Fig. S1D). This concentration of TMZ was previously defined by other groups as the dose able to distinguish sensitive vs resistant GSC cultures [12,13]. The expression levels of the main known TMZ resistance factor, MGMT—as assessed by RNA-seq (ref. [3])—are either absent or extremely low in our GSC models (Suppl. Table 1) and therefore do not correlate with TMZ sensitivity. Nonetheless, it is well established that, following TMZ treatment, GBM cells, and particularly GSCs, can activate alternative drug resistance mechanisms [14,15], which may account for the pronounced resistance observed in our models. A key aspect which contributes to cancer stem cell malignancy is their extreme ability to recover from DNA damage. We then utilized a higher dosage of TMZ (500 μM) to ensure efficient induction of DNA breaks in both shC and shMEOX2 cells, and performed alkaline comet assays to measure the ability of cells to repair DNA. Indeed, immediately after exposure to TMZ, DNA damage was observed in both shC and shMEOX2 cells, and the effect was significantly more pronounced in shMEOX2 cells, confirming our previous findings about the increased sensitivity of MEOX2 KD cells (Fig. 1E and Fig. S1E). At 24 h post-treatment, comet tail lengths in shC cells returned to baseline levels, comparable to untreated conditions, indicating efficient DNA repair. In contrast, shMEOX2 cells exhibited persistently longer DNA tails at the same time point, suggesting unresolved DNA damage and a defect in DNA repair mechanisms. We then asked if this defect in DNA repair of MEOX2 KD cells could be observed after ionizing radiation (IR) treatment too. We exposed shMEOX2 and shC cells to 2 Gy, collected them after 24h and 48h, checked the efficient induction of DNA damage in both shC and shMEOX2 cells (as shown by phospho-KAP1 increase, and subsequent decrease, Fig. S1F), and assessed DNA repair by quantifying for γH2AX/53BP1 co-localized foci. As evident from Fig. 1F, we detected more foci per cell at 24 h than at 48 h, indicating that the DNA repair processes were still active between these two times in both shC and shMEOX2 cells. However, at both time points, we found more foci in shMEOX2 cells compared to shC and, even more interestingly, after 48 h, shMEOX2 cells still showed a high number of foci, while shC cells returned to the basal level. Thus, DNA damage was still present in shMEOX2 cells, whose repair ability is reduced.

To better understand Meox2 function and the molecular mechanisms in which it is involved, we assessed the Meox2 protein interactome by co-immunoprecipitation (co-IP) experiments followed by mass spectrometry analysis. By immunoprecipitating endogenous Meox2 in BT273 GSCs, we found that one of the principal interactors is poly ADP-ribose polymerase1 (PARP1), a member of the PARP family. PARP1 is involved in maintenance of genome integrity and the repair of DNA damage [6]. After confirming the Meox2–PARP1 interaction in three additional GSC lines via co-IP of the endogenous proteins (Fig. 2A, Fig. S2A), we further validated this interaction by performing the reverse co-IP by immunoprecipitating PARP1 and searching for Meox2 (Fig. 2B). We corroborated this finding by using the AlphaFold2-multimer prediction tool, which estimated the likely involvement of the PADR1 domain of PARP1 (PARP1225–359) in the interaction with Meox2 homeodomain (Fig. 2C). We therefore compared the ability of recombinant wild-type Meox2 and a mutant form of Meox2 lacking the homeobox domain [16], to bind PARP1. We transfected HEK293T cells, which do not express endogenous MEOX2, with the two constructs and carried out co-IP experiments. These experiments showed that the homeobox domain is required for the interaction (Fig. 2D). As the homeobox works as a DNA-binding domain, we reasoned that a

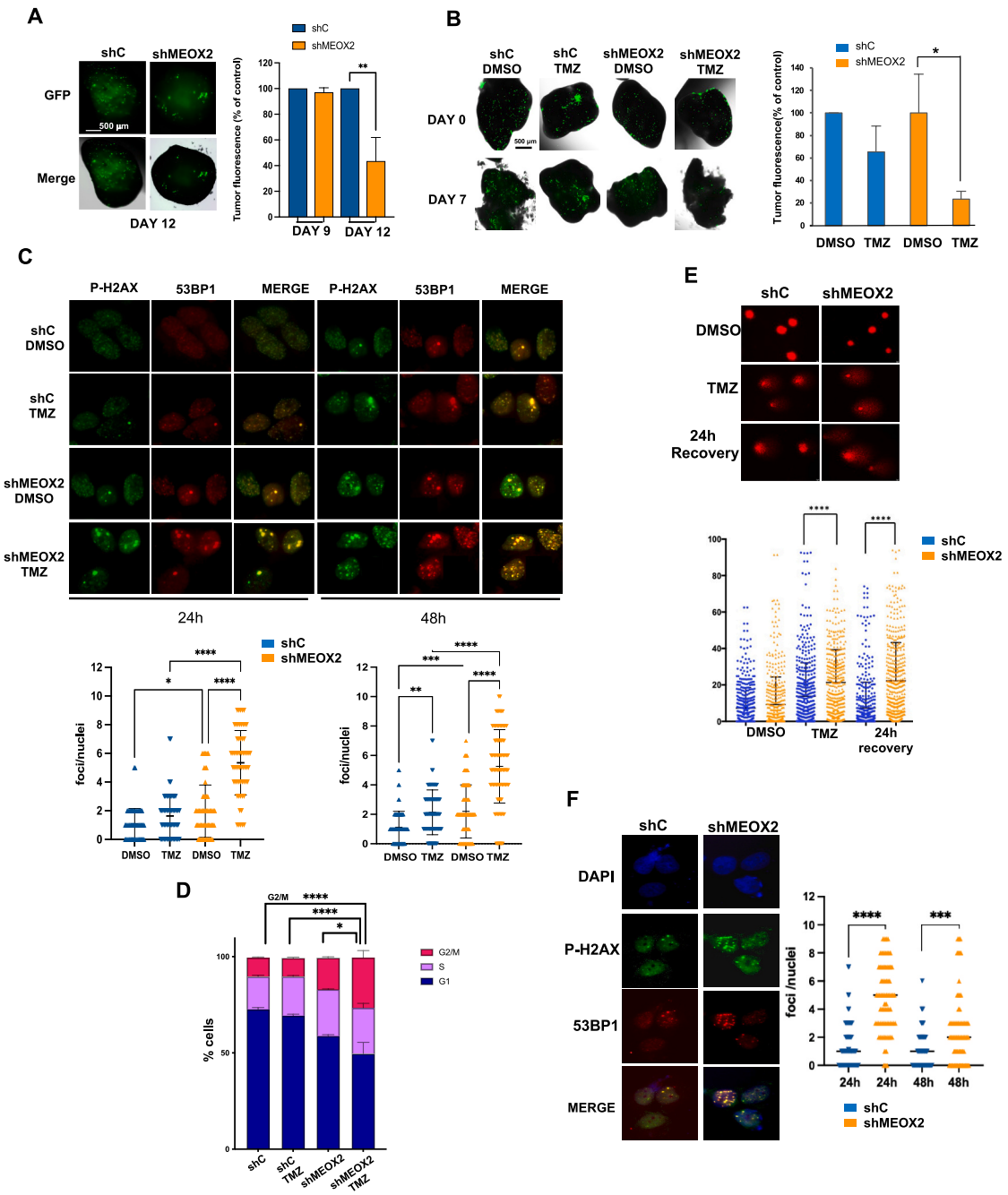


**Fig. 1.** MEOX2 Knockdown Impairs Tumour Growth, Enhances DNA Damage, and Sensitizes GSCs to TMZ-Induced G2/M Arrest

(A) Representative fluorescent microscopic images of control (shC) and MEOX2 knock-down (shMEOX2) tumor growth (left), and quantification (right) of GFP-expressing BT379 cells [3] in GLICO models after 12 days of growth; green, GFP; n = 6 organoids; scale bar, 500 μm

(B) Representative fluorescent microscopic images (left), and quantification (right) of GFP-expressing shC and shMEOX2 BT379 cells in GLICO models treated with 100 μM of TMZ; n = 6 organoids per group; scale bar, 500 μm

(C) Representative fluorescent microscopic images of shC and shMEOX2 BT379 cells treated with 100 μM of TMZ for 24h and subsequently analyzed for phospho-H2AX and 53BP1 foci by immunofluorescent staining with anti-53BP1 (red) and anti-Phospho-H2AX (Ser139, green) antibodies. Bar graphs show the number of γH2AX/53BP1 foci per nucleus counted on >80 cells. DAPI was used for nuclear staining. The co-localization of the two antibodies was used to measure DNA double-strand breaks counted on >80 cells (bar graph).

(D) Cell cycle analysis of shC and shMEOX2 BT379 cells after 24h TMZ treatment (100 μM). DAPI staining shows G2/M accumulation in shMEOX2 after TMZ treatment compared to shC control.

(E) Representative images of alkaline comet assay in shC and shMEOX2 BT379 cells treated with 500 μM of TMZ for 24h, followed by 24h recovery in fresh medium without drug. DNA damage was quantified via the percentage DNA in tails (bar graph).

(F) Representative immunofluorescence images of shC and shMEOX2 BT273 cells 24h after IR (2 Gy) treatment. DNA damage was evaluated as in (C) by γH2AX and 53BP1 co-staining. Bar graphs show the number of γH2AX/53BP1 foci per nucleus counted on >100 cells, at 24h and 48h after treatment.

Results were verified from three independent experiments and analyzed using GraphPad Prism 10. mean ± SD. A-B two-tailed Student's *t*-test. C-F two-way ANOVA test. *p < 0.05, **p < 0.01, ***p < 0.001, and ****p < 0.0001. (For interpretation of the references to color in this figure legend, the reader is referred to the Web version of this article.)

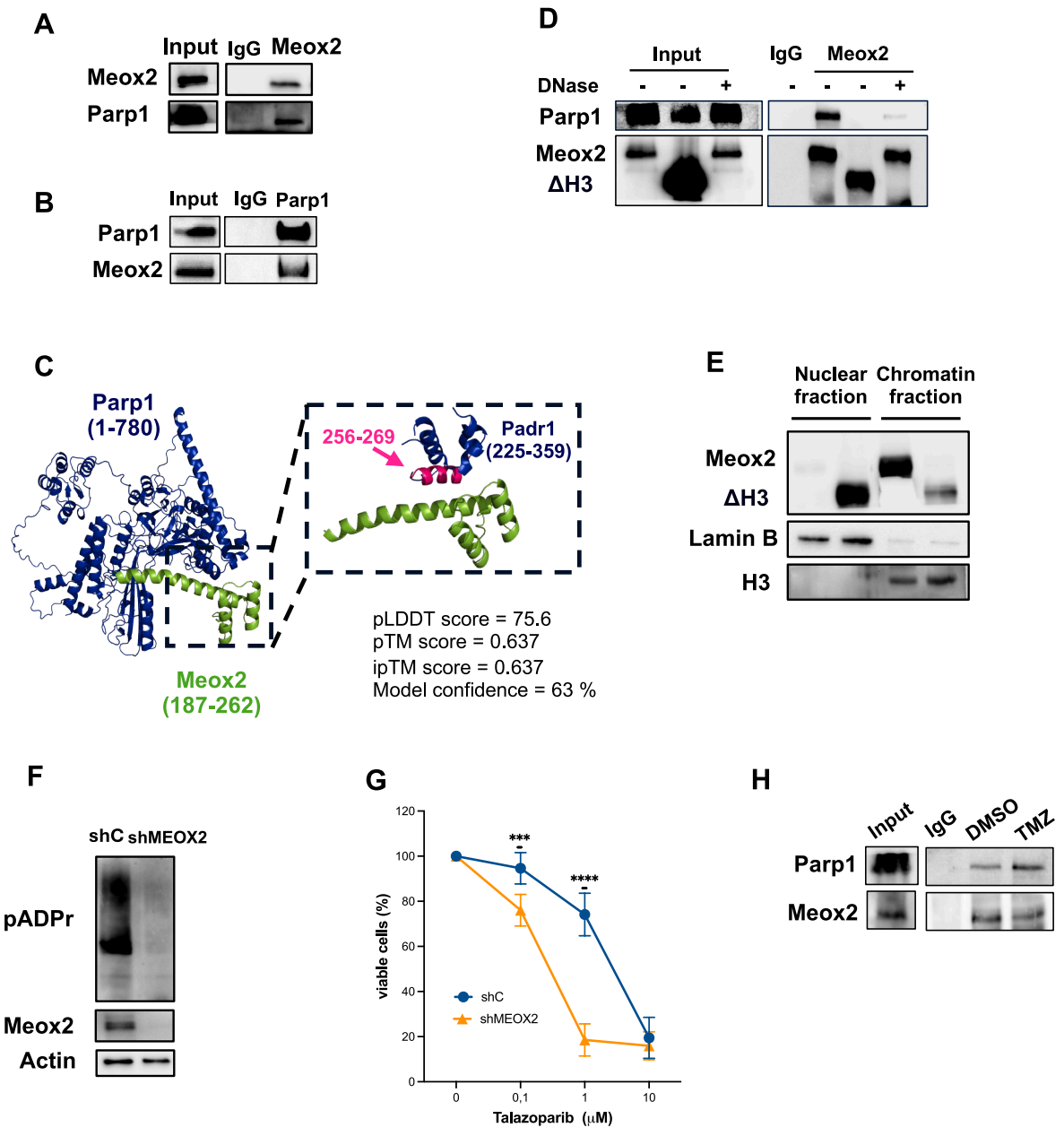


**Fig. 2.** Meox2 interacts with PARP1 and promotes Talazoparib Resistance in Glioblastoma Stem Cells

(A) Cell lysates from BT379 (Input) were analyzed by IP using antibodies against Meox2, then subjected to IB analysis to verify the interaction between Meox2 and PARP1. IgG was used as the isotype negative control.

(B) Cell lysates from BT273 (Input) were analyzed by IP using antibodies against PARP1, then subjected to IB analysis as in A.

(C) The computational model illustrates the interaction between a selected segment of PARP1 (residues 1–780, representing the full-length protein devoid of its catalytic domain, depicted in blue) and the homeodomain of Meox2 (residues 187–262, shown in green). The prediction corroborates the involvement of the PADR1 domain of PARP1 ($PARP1^{225-359}$) and a precise interacting sequence, i.e. CSTNDLKELLIFNK, was identified ($PARP^{256-269}$, pink domain on the zoom view). Each protein was distinguished by coloration. Protein-protein interaction was determined using Modify/Around/Atoms within 4 Å.

(D) Two constructs—one harboring the recombinant wild-type MEOX2 (Meox2) and the other a mutant MEOX2 lacking the homeobox domain (ΔHB)—were transfected into HEK-293T cells (Input). Cell lysates were subjected to IP using anti-Meox2 antibodies, with or without DNase treatment, followed by IB analysis.

(E) Representative image of IB analysis of recombinant wild-type Meox2 (Meox2) or a mutant Meox2 lacking the homeobox domain (ΔHB) present in nuclear and chromatin fractions of HEK-293T cells. Lamin B represents the nuclear fraction marker while histone H3 represents the chromatin fraction marker. Ectopic expression experiments were performed by transient transfections, and analyzed at 48h post-transfection. Results were verified from three independent experiments.

(F) Cell lysates from shC and shMEOX2 BT379 cells were analyzed by IB using antibodies against the indicated antibodies.

(G) shC and shMEOX2 BT379 cells were treated for 72 h h with increasing concentrations of Talazoparib. Cell viability was assessed using the fluorescein diacetate (FDA) staining and analyzed by flow cytometry.

(H) Chromatin-associated proteins from BT379 cells, treated or untreated with 100 μM TMZ, were immunoprecipitated with Meox2 antibodies and analyzed by immunoblotting to detect Meox2–PARP1 interaction. IgG was used as a negative control.

Results were verified from three independent experiments. mean ± SD. two-way ANOVA test. ***$p < 0.001$, ****$p < 0.0001$. (For interpretation of the references to color in this figure legend, the reader is referred to the Web version of this article.)

protein interaction which involves the homeodomain, likely involves DNA to occur. In line with this hypothesis, DNase I treatment of the samples in the co-IP experiments almost abolished the interaction of PARP1 and Meox2 (Fig. 2D). Indeed, the Meox2 homeodomain is needed for DNA binding by Meox2, as confirmed by the fact that we found the wild-type form of Meox2 in the chromatin fraction but not the mutant form (Fig. 2E).

Since PARP1 enzymatic activity is critical for DNA damage repair via poly-ADP-ribosylation, we examined whether MEOX2 knockdown affects this PARP1 function. In shMEOX2 cells, we found a marked decrease in overall cellular PARylation (Fig. 2F, Fig. S2B), indicating reduced PARP1 activity. These findings suggested to us that MEOX2 KD, through reducing PARP1 PARylation activity, might sensitize cells to PARP1 inhibition. When we compared the overall survival of shC and shMEOX2 cells treated with the PARP1 inhibitor Talazoparib, MEOX2 knockdown significantly enhanced the drug's cytotoxic effect. Notably, this increased sensitivity was evident at drug concentrations that could not affect the viability of shC cells (Fig. 2G, Fig. S2C). Thus, as for TMZ, the reduction of MEOX2 renders GSCs more sensitive to drug dosages which do not affect control cells. Our results unveil a totally new role for Meox2 in GSCs, which are considered responsible for initiation and above all for therapy resistance of glioblastoma. We provide novel insights about Meox2 involvement in the ability of GSCs to repair DNA damage upon chemo- (TMZ) and radiotherapy. By demonstrating the functional interaction with PARP1, we uncover a new mechanism through which Meox2 works as a critical regulator of DNA repair and therapeutic resistance in GSCs. We believe that our findings may, at least in part, explain observations reported in several studies that analyzed MEOX2 expression in public glioblastoma datasets (TCGA and CGGA). These studies identified MEOX2 as an important prognostic factor [17,18], consistently showing its overexpression across all glioma subtypes compared with healthy brain tissue, a negative correlation between MEOX2 expression and patient survival, and an enrichment of MEOX2 expression in GBM patients who do not respond to radiotherapy [2,15,18,19]. In addition, our results shed a mechanistic light onto some previous observations linking MEOX2 not merely to glioblastoma growth, but specifically to the response to chemotherapy via alkylating agents and to radiotherapy [2,20]. This of course does not exclude that Meox2 may act, in some GSC types, also via additional mechanisms, such as the transcriptional regulation of genes whose products are engaged in DNA repair. Nonetheless, we think that this does not change the novelty and potential importance of our present work.

From a mechanistic point of view, our findings raise the question about how Meox2-PARP1 interaction works in modulating DNA damage. When we measured PARP1 stability in a cycloheximide chase assay, we did not detect any difference between shMEOX2 and shC cells (Fig. S2D), suggesting that Meox2 does not work merely by stabilizing PARP1. In light of our data, showing a reduction of parylation activity upon Meox2 KD, an intriguing hypothesis might be that Meox2 helps PARP1 in its recruitment to DNA damage sites. Our structural prediction pointing at the chromatin binding PADR domain of PARP1 as the likely interaction site with Meox2, might be in agreement with a model where Meox2 contributes to PARP1 binding to damaged DNA. In agreement with this hypothesis, when we immunoprecipitated Meox2 specifically in the chromatin fraction, and searched for PARP1 in either untreated or TMZ (100 μM) treated cells, we found that TMZ induced an increased amount of PARP1 co-immunopreciptating with Meox2 (Fig. 2H).

The physical and functional link with PARP1 also raises the intriguing possibility that reducing MEOX2 might help overcome the resistance to PARP1 inhibitors often shown by glioblastomas, particularly in their recurrence.

A limitation of our present work is the lack of experiments with tumor xenografts. However, by this study, we aim at providing the proof of principle about Meox2 involvement in DNA damage repair in GBM, while we believe that a larger, dedicated work needs to be performed in the much more complex conditions of orthotopic xenografts, where the interactions with microenvironment might modulate the results we are now showing.

While we acknowledge that the TMZ doses we employed in our experiments are above the ≤50 μM range requested in a real clinical setting, we highlight the mechanistic value of the results we obtained, as we think they may set the premises for perspective studies aimed at determining if targeting the MEOX2–PARP1 axis may represent a promising strategy to sensitize resistant GSCs and improve therapeutic responses in GBM.

## CRediT authorship contribution statement

**Monia Russo:** Writing – review & editing, Validation, Methodology, Investigation, Formal analysis, Data curation. **Elvia Valentini:** Writing – review & editing, Validation, Methodology, Investigation, Formal analysis, Data curation. **Vincenza Aliperti:** Validation, Methodology, Formal analysis. **Federico Copparoni:** Validation, Methodology, Investigation, Formal analysis. **Amanda Linkous:** Writing – review & editing, Validation, Resources, Methodology, Investigation, Formal analysis. **Claudia Montaldo:** Resources, Methodology, Investigation, Formal analysis. **Silvia Soddu:** Supervision, Resources. **Jean-Maxime Besson:** Writing – review & editing, Methodology, Formal analysis. **Marie Lopez:** Writing – review & editing, Methodology, Formal analysis. **Manuela Helmer Citterich:** Writing – review & editing, Funding acquisition. **Alessandro Michienzi:** Writing – review & editing, Funding acquisition. **Marco Tripodi:** Writing – review & editing, Funding acquisition. **Silvia Anna Ciafrè:** Writing – review & editing, Writing – original draft, Supervision, Project administration, Methodology, Funding acquisition, Formal analysis, Conceptualization. **Silvia Galardi:** Writing – review & editing, Supervision, Project administration, Methodology, Funding acquisition, Formal analysis, Conceptualization.

## Ethical approval and consent to participate

All patients gave written informed consent to use the samples for experiments, and for the results derived thereof to be published (protocol n. FINCB CI25). Processing of the BT human GSC lines was approved by the institutional Ethical Committee of Fondazione IRCCS Istituto Neurologico C. Besta (FINCB). All study methodologies were in line with the standards outlined in the Declaration of Helsinki.

## Funding

This research was funded by 'Fondazione Giovanni Celeghin'; by European Union—NextGenerationEU: National Center for Gene Therapy and Drugs based on RNA Technology, CN3—Spoke 7 (code: CN00000041; PNRR—Mission 4, Component 2; Investment 1.4); AIRC IG 23539; AIRC IG 26290, PRIN 2022 2022ETPX42.

## Declaration of competing interest

The authors declare that this manuscript is original, has not been published before and is not currently under consideration for publication elsewhere.

There are no conflicts of interest associated with this publication, and there has been no financial support to this work that could have influenced its outcome.

## Acknowledgements

We thank Maria Pia Gentileschi (IRCCS Regina Elena Cancer Institute) for technical support with the gamma-irradiator.

## Appendix A. Supplementary data

Supplementary data to this article can be found online at https://doi.

org/10.1016/j.canlet.2026.218284.

## References


[1] L.R. Schaff, I.K. Mellinghoff, Glioblastoma and other primary brain malignancies in adults: a review, JAMA 329 (7) (2023 Feb 21) 574–587, https://doi.org/10.1001/jama.2023.0023.

[2] F. Ducray, A. de Reyniès, O. Chinot, A. Idbaih, D. Figarella-Branger, C. Colin, L. Karayan-Tapon, H. Chneiweiss, M. Wager, F. Vallette, et al., An ANOCEF genomic and transcriptomic microarray study of the response to radiotherapy or to alkylating first-line chemotherapy in glioblastoma patients, Mol. Cancer 9 (2010) 234, https://doi.org/10.1186/1476-4598-9-234.

[3] C. Proserpio, S. Galardi, M.G. Desimio, A. Michienzi, M. Doria, A. Minutolo, C. Matteucci, S.A. Ciafrè, MEOX2 regulates the growth and survival of glioblastoma stem cells by modulating genes of the glycolytic pathway and response to hypoxia, Cancers (Basel) 14 (9) (2022 May 6) 2304, https://doi.org/10.3390/cancers14092304.

[4] A. Schönrock, E. Heinzelmann, B. Steffl, E. Demirdizen, A. Narayanan, D. Krunic, M. Bähr, J.W. Park, C. Schmidt, K. Özduman, M.N. Pamir, W. Wick, F. Bestvater, D. Weichenhan, C. Plass, J. Taranda, M. Mall, Ş. Turcan, MEOX2 homeobox gene promotes growth of malignant gliomas, Neuro Oncol. 24 (11) (2022 Nov 2) 1911–1924, https://doi.org/10.1093/neuonc/noac110.

[5] A.R. Sloan, D.J. Silver, S. Kint, M. Gallo, J.D. Lathia, Cancer stem cell hypothesis 2.0 in glioblastoma: where are we now and where are we going? Neuro Oncol. 26 (5) (2024 May 3) 785–795, https://doi.org/10.1093/neuonc/noae011.

[6] D. Huang, W.L. Kraus, The expanding universe of PARP1-mediated molecular and therapeutic mechanisms, Mol. Cell 82 (12) (2022 Jun 16) 2315–2334, https://doi.org/10.1016/j.molcel.2022.02.021.

[7] A. Linkous, D. Balamatsias, M. Snuderl, L. Edwards, K. Miyaguchi, T. Milner, B. Reich, L. Cohen-Gould, A. Storaska, Y. Nakayama, E. Schenkein, R. Singhania, S. Cirigliano, T. Magdeldin, Y. Lin, G. Nanjangud, K. Chadalavada, D. Pisapia, C. Liston, H.A. Fine, Modeling patient-derived glioblastoma with cerebral organoids, Cell Rep. 26 (12) (2019 Mar 19) 3203–3211.e5, https://doi.org/10.1016/j.celrep.2019.02.063.

[8] A.R. Pine, S.M. Cirigliano, J.G. Nicholson, Y. Hu, A. Linkous, K. Miyaguchi, L. Edwards, R. Singhania, T.H. Schwartz, R. Ramakrishna, D.J. Pisapia, M. Snuderl, O. Elemento, H.A. Fine, Tumor microenvironment is critical for the maintenance of cellular states found in primary glioblastomas, Cancer Discov. 10 (7) (2020 Jul) 964–979, https://doi.org/10.1158/2159-8290.CD-20-0057.

[9] M.S. Tomar, A. Kumar, C. Srivastava, A. Shrivastava, Elucidating the mechanisms of temozolomide resistance in gliomas and the strategies to overcome the resistance, Biochim. Biophys. Acta Rev. Canc 1876 (2) (2021) 188616, https://doi.org/10.1016/j.bbcan.2021.188616.

[10] J. Williamson, C.M. Hughes, G. Burke, G.W. Davison, A combined γ-H2AX and 53BP1 approach to determine the DNA damage-repair response to exercise in hypoxia, Free Radic. Biol. Med. 154 (2020 Jul) 9–17, https://doi.org/10.1016/j.freeradbiomed.2020.04.026.

[11] Y. Hirose, M.S. Berger, R.O. Pieper, p53 effects both the duration of G2/M arrest and the fate of temozolomide-treated human glioblastoma cells, Cancer Res. 61 (5) (2001 Mar 1) 1957–1963.

[12] I. Ntafoulis, A. Kleijn, J. Ju, K. Jimenez-Cowell, F. Fabro, M. Klein, R.T. Chi Yen, R. K. Balvers, Y. Li, A.P. Stubbs, T.V. Kers, J.M. Kros, S.E. Lawler, L.V. Beerepoot, A. Kremer, A. Idbaih, M. Verreault, A.T. Byrne, A.C. O'Farrell, K. Connor, A. Biswas, M. Salvucci, J.H.M. Prehn, D. Lambrechts, G. Dilcan, F. Lodi, I. Arijs, M. J. van den Bent, C.M.F. Dirven, S. Leenstra, consortium Gliotrain, M.L.M. Lamfers, Ex vivo drug sensitivity screening predicts response to temozolomide in glioblastoma patients and identifies candidate biomarkers, Br. J. Cancer 129 (8) (2023 Oct) 1327–1338, https://doi.org/10.1038/s41416-023-02402-y.

[13] A.B. Díaz Méndez, M. Di Giuliani, A. Sacconi, E. Tremante, V. Lulli, M. Di Martile, G. Vari, F. De Bacco, C. Boccaccio, G. Regazzo, M.G. Rizzo, Androgen receptor inhibition sensitizes glioblastoma stem cells to temozolomide by the miR-1/miR-26a-1/miR-487b signature mediated WT1 and FOXA1 silencing, Cell Death Discov. 11 (1) (2025 May 21) 248, https://doi.org/10.1038/s41420-025-02517-6.

[14] D. Beier, J.B. Schulz, C.P. Beier, Chemoresistance of glioblastoma cancer stem cells–much more complex than expected, Mol. Cancer 10 (2011 Oct 11) 128, https://doi.org/10.1186/1476-4598-10-128.

[15] J.L. McFaline-Figueroa, C.J. Braun, M. Stanciu, Z.D. Nagel, P. Mazzucato, D. Sangaraju, E. Cerniauskas, K. Barford, A. Vargas, Y. Chen, N. Tretyakova, J. A. Lees, M.T. Hemann, F.M. White, L.D. Samson, Minor changes in expression of the mismatch repair protein MSH2 exert a major impact on glioblastoma response to temozolomide, Cancer Res. 75 (15) (2015 Aug 1) 3127–3138, https://doi.org/10.1158/0008-5472.CAN-14-3616. Epub 2015 May 29. PMID: 26025730.

[16] E. Salichs, A. Ledda, L. Mularoni, M.M. Albà, S. de la Luna, Genome-wide analysis of histidine repeats reveals their role in the localization of human proteins to the nuclear speckles compartment, PLoS Genet. 5 (3) (2009 Mar) e1000397, https://doi.org/10.1371/journal.pgen.1000397.

[17] Q. Cheng, C. Huang, H. Cao, J. Lin, X. Gong, J. Li, Y. Chen, Z. Tian, Z. Fang, J. Huang, A novel prognostic signature of transcription factors for the prediction in patients with GBM, Front. Genet. 10 (2019 Oct 1) 906, https://doi.org/10.3389/fgene.2019.00906.

[18] W. Wu, W. Liu, Z. Liu, X. Li, Construction of a genetic prognostic model in the glioblastoma tumor microenvironment, Genes 16 (8) (2025 Jul 24) 861, https://doi.org/10.3390/genes16080861.

[19] G. Tachon, K. Masliantsev, P. Rivet, C. Petropoulos, J. Godet, S. Milin, M. Wager, P. O. Guichet, L. Karayan-Tapon, Prognostic significance of MEOX2 in gliomas, Mod. Pathol. 32 (6) (2019 Jun) 774–786, https://doi.org/10.1038/s41379-018-0192-6.

[20] T. Li, K. Sun, W. Yang, M. Zhang, W. Feng, S. Chen, M. Zuo, Q. Yuan, Y. Liu, M. Chen, MEOX2 promotes glioma growth and temozolomide chemoresistance, J. Pharm. Anal. 14 (9) (2024 Sep) 100912, https://doi.org/10.1016/j.jpha.2023.12.002.